Indian J. Phys. **68B** (4), 321–332 (1994)

IJP B
— an international journal

Triply and doubly differential cross sections in positron-impact ionization of atomic hydrogen

P K Dutta+, P Mandal+, K Roy and N C Sil

Department of Theoretical Physics, Indian Association for the Cultivation of Science, Jadavpur, Calcutta-700 032, India

+Department of Mathematics, Visva-Bharati University, Santiniketan-731 235, India

Received 24 November 1993, accepted 18 May 1994

Abstract : Positron-impact ionization of atomic hydrogen is considered using the Faddeev wave function for the final state. Results of the doubly and triply differential cross sections are obtained with a view to studying the case when the excess energy in the final channel is almost equally shared by the electron and the positron. The Faddeev differential cross section exhibits a cusp-shape at the lower incident energies of positron impact, while a hump in the cross section is obtained at higher energies beyond 150 eV. The observed data on the other hand, for the positron-argon system at 100 eV, do not show the predicted cusp-shape. The present results are compared with those obtained by the plane-wave Born approximation.

Keywords : Positron, ionization, Faddeev wavefunction, Born approximation

PACS Nos. : 34.80.Dp, 34.50.Fa

1. Introduction

In an earlier work [1], we reported briefly the results of our study on the positron-impact ionization of atomic hydrogen using the final-state wavefunction as obtained from the three body scattering formalism of Faddeev [2]. We showed the relative importance of the two competing processes involved in the scattering mechanism, namely, (a) the direct ionization with the emission of the electron relative to the residual proton and (b) the electron-capture to the continuum state of the positron (*i.e.* positronium formation in the continuum). Our calculation predicts a cusp in the forward doubly differential cross section when the excess energy in the exit channel is equally shared by the scattered positron and the emitted electron. At these energies the continuum electron is carried along by the scattered positron in the forward direction, as a result of which there is a sharp peak of the triply differential cross section near the forward angle. This phenomenon is present in all such reactions of chargetransfer to the continuum in ion-atom collisions and has been extensively studied both theoretically [3–7] and experimentally [8–11]. For positron scattering, however, there has been no experimental verification of our predictions as yet. Nonetheless, Brauner and Briggs [12] have obtained similar results by considering the first-order Born matrix element where the final-state is described by the positron and ionized electron in a Coulomb eigenstate of their relative momentum. In analogy with ion-atom collision, they have however taken the interaction potential to be either the positron-electron or the electron-target nucleus interaction in their calculations. Using the classical trajectory Monte Carlo technique, Schultz and Reinhold [13] have further obtained a ridge-like structure instead of the cusp-shape in the doubly differential cross section near the forward angle and have demonstrated that the positron is readily deflected to large angles and suffers substantial energy loss in the cross section. Recently, Brauner *et al* [14] have used a final-state wavefunction as the product of three Coulomb wavefunctions satisfying appropriate boundary conditions and have evaluated the matrix element following the method of Roy *et al* [15]. The direct ionization process (a) has however, been studied by many authors using different methods including the second Born approximation [16]. The recent measurements by the University College, London group [17] on the double-differential cross section for the e^+-Ar system, do not show the cusp-shape as discussed earlier [1]. Instead a ridge-like structure is observed similar to that predicted by Schultz and Reinhold [13].

The purpose of the present paper is to give the details of our earlier calculation using Faddeev's theory [1] and to report the dramatic behaviour of the triply and doubly differential cross sections at various incident positron and ejected electron energies. It is to be emphasized that our previous work was primarily concerned with the establishment of the importance of the electron-capture to the continuum in positron-impact ionization of atoms (and molecules). Our main attention had there been to study the energy region where the emitted electron and the scattered positron shared almost equal energy in the final channel. In the present work, we study the cusp-structure in great detail and report new results of the doubly differential cross section as a function of the electron emission energy at the forward emission angle for several incident energies. For two incident positron energies however, we have also made calculations for the Weigold symmetric geometry.

2. The scattering amplitude and its evaluation

We consider the incident positron, the atomic electron and the proton as particles 1, 2 and 3 respectively with their masses, position coordinates and momenta given by m_i, r_i and k_i, $i = 1$ to 3. The relative and center-of-mass coordinates of the particles i, j are defined by $\boldsymbol{R}_{ij} = \boldsymbol{r}_i - \boldsymbol{r}_j$ and $\boldsymbol{S}_{ij} = (m_i \boldsymbol{r}_i + m_j \boldsymbol{r}_j)/(m_i + m_j)$, with their conjugate momenta $\boldsymbol{x}_{ij}$, $\boldsymbol{q}_{ij}$ respectively.

The transition matrix element is

$$T_{if}^{-} = \left\langle \Psi_f^{-} \middle| V_i \middle| \Psi_i \right\rangle, \tag{1}$$

where the Faddeev three-body wavefunction of the final-state for an ionizing collision is given by [2]

$$\Psi_f^- = \Phi + \psi^{(1)} + \psi^{(2)} + \psi^{(3)} \tag{2}$$

The plane-wave state Φ denotes the situation when all the particles are asymptotically free and

$$\Phi = (2\pi)^{-9/2} \exp\left[i \sum^{3} \boldsymbol{k}_\alpha \cdot \boldsymbol{r}_\alpha \right]. \tag{3}$$

The components $\Psi^{(1)}$, $\Psi^{(2)}$, $\Psi^{(3)}$ satisfy the integral equation

$$\begin{pmatrix} \Psi^{(1)} \\ \Psi^{(2)} \\ \Psi^{(3)} \end{pmatrix} = \begin{pmatrix} \Phi^{(23)} - \Phi \\ \Phi^{(31)} - \Phi \\ \Phi^{(12)} - \Phi \end{pmatrix} - G_0^+ \begin{pmatrix} 0 & T_{23} & T_{23} \\ T_{31} & 0 & T_{31} \\ T_{12} & T_{12} & 0 \end{pmatrix} \begin{pmatrix} \Psi^{(1)} \\ \Psi^{(2)} \\ \Psi^{(3)} \end{pmatrix} \tag{4}$$

T_{ij} are the two-body t-matrix elements for the particles i and j. $\Phi^{(ij)}$ are the solutions of the two-particle subsystems interacting *via* potentials $V_{ij}\left(\left|\boldsymbol{r}_i - \boldsymbol{r}_j\right|\right)$ with the boundary condition that they approach the plane wave state (3) for large separations of all the particles and are given as [1,4]

$$\Phi^{(ij)} = (2\pi)^{-3} \exp\left[i\left(\boldsymbol{k}_\alpha \cdot \boldsymbol{r}_\alpha + \boldsymbol{q}_{ij} \cdot \boldsymbol{s}_{ij} \right) \right] \Psi_{x_{ij}}^- (\boldsymbol{R}_{ij}). \tag{5}$$

Here $\Psi_{x_{ij}}^- (\boldsymbol{R}_{ij})$ denote the Coulomb wave functions of particles i and j with their relative momenta $\boldsymbol{x}_{ij}$ and are obtained as [18]

$$\Psi_{x_{ij}}^- = N_f(x_{ij}) \exp\left(i\boldsymbol{x}_{ij} \cdot \boldsymbol{R}_{ij} \right) {}_1F_1\left(in_{ij}; 1; -ix_{ij}R_{ij} - i\boldsymbol{x}_{ij} \cdot \boldsymbol{R}_{ij} \right) \tag{6}$$

with

$$\begin{aligned} N_f(x_{ij}) &= (2\pi)^{-3/2} \exp\left(-\pi n_{ij}/2 \right) \Gamma\left(1 - in_{ij} \right), \\ n_{ij} &= \alpha_{ij}/x_{ij}\,;\ \alpha_{ij} = m_{ij} Z_i Z_j \ \text{(a.u)}, \\ m_{ij} &= m_i m_j/(m_i + m_j);\ Z_1 = Z_3 = 1,\ Z_2 = -1. \end{aligned} \tag{7}$$

G_0^+ is the Green's function for three non-interacting particles and the interaction potential $V_{\mathrm{int}} = V_2 + V_3$,

where

$$V_2 = 1/R_{13}, \quad V_3 = -1/R_{12} \ \text{(a.u)}.$$

The initial state of the positron-hydrogen atom system is described by

$$\Psi_i = (2\pi)^{-3} \exp\left[i\left(\mathbf{k}_i \cdot \mathbf{r}_1 + \mathbf{q}_i \cdot \mathbf{s}_{23}\right) \Phi_i(\mathbf{R}_{23})\right. \tag{8}$$

where $\Phi_i(\mathbf{R}_{23})$ stands for the wavefunction of normal hydrogen atom and is $N_i \exp(-\lambda_i R_{23})$, $N_i = \left(\lambda_i^3/\pi\right)^{1/2}$, $\lambda_i = 1$ (a.u) and $\mathbf{k}_i$, $\mathbf{q}_i$ are the initial values of the momentum.

We retain only the first-order term in eq. (4) and use it in eq. (2) to obtain

$$\Psi_f^- = \Phi^{(23)} + \Phi^{(31)} + \Phi^{(12)} - 2\Phi, \tag{9}$$

which on applying in eq. (1) yields

$$T_{fi}^- = t_{23} + t_{31} + t_{12} - 2t_0, \tag{10}$$

where

$$t_{jk} = \left\langle \Phi^{(jk)} \middle| V_{\text{int}} \middle| \Psi_i \right\rangle; \; t_0 = \left\langle \Phi \middle| V_{\text{int}} \middle| \Psi_i \right\rangle. \tag{11}$$

The matrix element t_{23} corresponds to the direct ionization process (a) and is also obtained in the usual Born approximation.

It has been given in closed analytic form by Massey and Mohr [19] and by Landau and Lifshitz [20] analytically.

The matrix element t_{12} corresponds to the electron-capture (or positronium formation) to the continuum and is written as the sum of two terms

$$t_{12}^{(1)} = \left\langle \Phi^{(12)} \middle| V_2 \middle| \Psi_i \right\rangle \text{ and } t_{12}^{(2)} = \left\langle \Phi^{(12)} \middle| V_3 \middle| \Psi_i \right\rangle.$$

Using the quantities $\mathbf{Q}_1 = \mathbf{x}_{21} - \mathbf{\Delta}$, $\mathbf{Q}_2 = \mathbf{\Delta} - \mathbf{x}_{23}$ where the momentum transfer vector $\mathbf{\Delta} = \mathbf{k}_i - \mathbf{k}_1$ (a.u) in the limit of infinite proton mass ($m_3 \to \infty$), we can express $t_{12}^{(1)}$ after carrying out the integration over $d\mathbf{s}_{23}$ as

$$t_{12}^{(1)} = (2\pi)^{-3} \delta\left(\mathbf{k}_i + \mathbf{q}_i - \mathbf{k}_3 - \mathbf{q}_{12}\right) \int e^{i\mathbf{Q}_1 \cdot \mathbf{R}_{21}} \times \Psi_{\mathbf{x}_{21}}^{-*}(\mathbf{R}_{21}) J(\mathbf{R}_{21}) d\mathbf{R}_{21}, \tag{12}$$

where the integral J is defined by

$$J(\mathbf{R}_{21}) = \int e^{i\mathbf{Q}_2 \cdot \mathbf{R}_{23}} V_2\left(\left|\mathbf{R}_{23} - \mathbf{R}_{21}\right|\right) \Phi_i(\mathbf{R}_{23}) d\mathbf{R}_{23} \tag{13}$$

and is expressed in closed form involving a single-dimensional integral from 0 to 1, which is shown in the Appendix. The final integration is carried out over the volume integral $d\mathbf{R}_{21}$ using the standard Nordsieck technique [21] to get

$$t_{12}^{(1)} = (2\pi)^{-3} \delta\left(\mathbf{k}_i + \mathbf{q}_i - \mathbf{k}_3 - \mathbf{q}_{12}\right) 8\pi^2 N_f^*(x_{21}) N_i \cdot \lambda_i \int^1 x dx L(x)/\mu, \tag{14}$$

where

$$\frac{L(x)}{\mu} = \left(\frac{1}{\mu}\frac{\partial}{\partial\mu}\right)^{2} \left(S_1/T_1\right)^{i\eta_{21}}/T_1, \tag{15}$$

$$T_1 = Q_3^2 + \mu^2, \tag{16}$$

$$S_1 = |Q_3 + x_{21}| - \left(x_{21} + i\mu\right)^2, \tag{17}$$

$$Q_3 = Q_1 - x_{21} - A. \tag{18}$$

It is to be noted that the integrand in the one-dimensional integral of eq. (14) is singular at $x = 0$. After the change of variable by the transformation $t = x^2$, this becomes free of singularity and the integral is then amenable to numerical evaluation. In order to evaluate $t_{12}^{(2)}$, we see that the integrals over ds_{23}, dR_{21} and dR_{23} are separable since the potential $V_3(R_{21})$ is a function of R_{21} alone. After performing integration over ds_{23}, we have as in eq. (12) an expression of the form

$$t_{12}^{(2)} = (2\pi)^{-3}\,\delta\left(k_i + q_i - k_3 - q_{12}\right) \int e^{iQ_1 \cdot R_{21}} \psi_{x_{21}}^{-*}(R_{21}) V_3(R_{21}) dR_{21}$$
$$\times \int e^{iQ_2 \cdot R_{23}}\, \Phi_i(R_{23}) dR_{23}. \tag{19}$$

The integration over dR_{21} is easily done following Nordsieck [21] and over dR_{23} by the Fourier integral transform method (as shown in the Appendix) to arrive at the final result

$$t_{12}^{(2)} = -(2\pi)^{-3}\,\delta\left(k_i + q_i - k_3 - q_{12}\right) \times 32\pi^2 N_f^*(x_{21})$$
$$\times N_i \lambda_i \left(S_2^0/T_2^0\right)^{i\eta_{21}} \Big/ \left[\left(Q_2^2 + \lambda_i^2\right)^2 T_2^0\right], \tag{20}$$

where

$$T_2^0 = |Q_1 - x_{21}|^2 = \Delta^2, \quad S_2^0 = Q_1^2 - x_{21}^2. \tag{21}$$

Our eq. (20) agrees with that given by Macek [4] for the corresponding element t_{12} in ion-atom collisions where the internuclear potential V_2 is neglected in the calculations of the transition matrix element, since it does not contribute to the scattering. These arguments are not readily applicable in the case of positron-atom collisions. The consideration of the kinematic translation from ion-atom collisions to positron-atom collisions does not seem plausible because of the enormous mass-difference between a positron (or an electron) and a proton [1].

The matrix element t_{31} is related to the case where the scattered positron moves in the continuum repulsive Coulomb field of the proton and is a natural outcome of the Faddeev equations. We have evaluated the elements $t_{31}^{(1)}$, $t_{31}^{(2)}$ by using the earlier methods in closed forms and are expressed as

$$t_{31}^{(1)} = (2\pi)^{-3}\,\delta(\boldsymbol{k}_i + \boldsymbol{q}_i - \boldsymbol{k}_2 - \boldsymbol{q}_{31})\,32\pi^2 N_f^*(x_{31})$$

$$\times N_i\lambda_i\left(S_3^0/T_3^0\right)^{i\eta_{31}}\Big/\left[\left(x_{23}^2+\lambda_i^2\right)^2 T_3^0\right], \tag{22}$$

$$t_{31}^{(2)} = -(2\pi)^{-3}\,\delta(\boldsymbol{k}_i + \boldsymbol{q}_i - \boldsymbol{k}_2 - \boldsymbol{q}_{31})\,8\pi^2 N_f^*(x_{31})$$

$$\times N_i\lambda_i \int_0^1 x dx L'(x)/\mu', \tag{23}$$

where

$$T_3^0 = \Delta^2,\; S_3^0 = k_i^2 - x_{31}^2, \tag{24}$$

$$T_1' = |\Delta - \Lambda'|^2 + \mu'^2, \tag{25}$$

$$S_1' = |\Delta - \Lambda + \boldsymbol{x}_{31}|^2 - (x_{31} + i\mu')^2, \tag{26}$$

$$\mu' = x\lambda_i^2 + x(1-x)\,x_{23}^2, \tag{27}$$

$$\Lambda = x\,x_{23}, \tag{28}$$

$$L' = \left(\frac{1}{\mu'}\frac{\partial}{\partial\mu'}\right)^2 \left[\left(S_1'/T_1'\right)^{i\eta_{31}}/T_1\right]. \tag{29}$$

Finally, the matrix element t_0 is obtained in a straight forward manner in the limit of infinite proton mass $m_3 \to \infty$ by using the Fourier integral transforms as

$$t_0 = (2\pi)^{-9/2}\,\delta(\Delta + \boldsymbol{q}_i - \boldsymbol{k}_2 - \boldsymbol{k}_3)\,32\pi^2 N_i\lambda_i\left[\left(x_{23}^2 + \lambda_i^2\right)^{-2}\right.$$

$$\left. - \left(Q_2^2 + \lambda_i^2\right)^{-2}\right]\Big/\Delta^2 \tag{30}$$

these matrix elements are then used in eq. (10) to compute the cross sections.

3. Results and discussions

A. *Triply differential cross section (TDCS) :*

In suitably chosen polar coordinates we have $\boldsymbol{k}_i = (k_i, 0, 0)$, $\boldsymbol{k}_1 = (k_1, \theta_1, 0)$, $\boldsymbol{k}_2 = (k_2, \theta_2, \Phi)$ where θ_1 is the angle between the incident positron and the ejected electron, and Φ is the difference in azimuth between $\boldsymbol{k}_1$ and $\boldsymbol{k}_2$. Using eq. (10), computations have been performed for the triply differential cross section for different sets of values of the above quantities. We have used the Gauss-Legendre quadrature method to evaluate the single-dimensional integral in the scattering matrix.

At intermediate incident positron energies E_i = 50, 80 and 300 eV, the values of the triply differential cross section are obtained for positron scattering angle $\theta_1 = 4°$ with

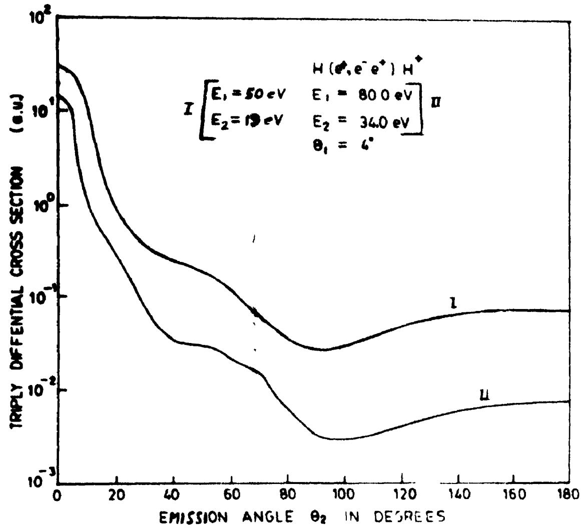

Figure 1. TDCS obtained by Faddeev formalism as a function of the ejection angle θ_2 for $H(e^+, e^- e^+)H^+$ collisions. The calculations are performed for $\theta_1 = 4°$ and $\Phi = 180°$ whereas set I : $E_i = 50$ eV, $E_2 = 19$ eV
set II : $E_i = 80$ eV, $E_2 = 34$ eV

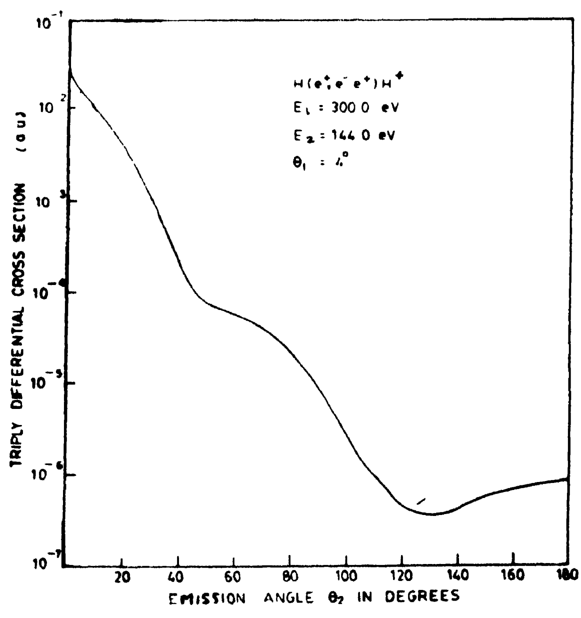

Figure 2. Same as Figure 1 except $E_i = 300$ eV and $E_2 = 144$ eV.

$\Phi = 180°$ as a function of the emission angle. These calculations are performed for ejected electrons having energy almost equal to the scattered positrons. Figures 1 and 2 display these results. It is evident from the figures that the ejected electron is almost carried along in the forward direction, thereby displaying a peaking of the cross section at these angles. This signifies the importance of the electron capture to the continuum process in positron-atom ionization collisions when the excess energy available in the exit channel is almost equally shared by the emerging particles. When the ejected electron's energy is much higher (*i.e.* when Δ is large) as in Figure 2, the results of our calculation for the ionization including the effect of capture to the continuum are in qualitative agreement with the direct ionization results, though differing in quantitative numerical values.

The results of the triply differential cross section for the symmetric Weigold geometry when $\theta_1 = \theta_2 = \theta$ and $k_1 = k_2 = k$ are shown in Figure 3 for only two incident energies E_i = 100 eV and 300 eV. Since in this case the emitted electron and the scattered positron have equal energies in the final channel, the electron capture to the continuum becomes rather dominant in the ionization process. This is evident from the sharp forward peaking of the Faddeev cross section which implies that the ejected electron is in fact carried along by the

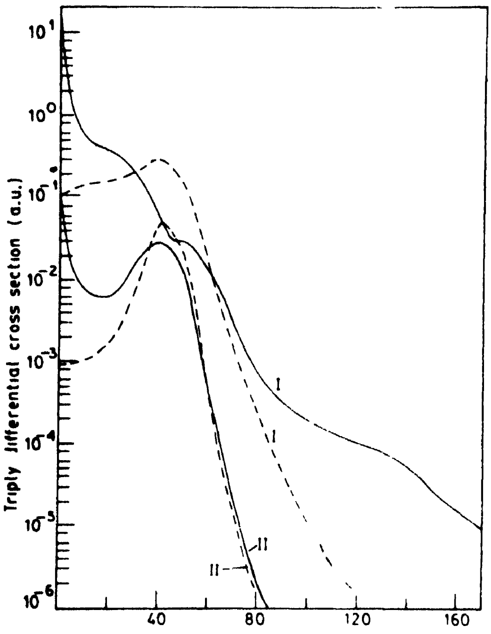

Figure 3. Same as Figure 1 except for $\theta_1 = \theta_2$ and
set I : $E_i = 100$ eV, $E_2 = 43.2$ eV
set II : $E_i = 300$ eV, $E_2 = 143.2$ eV.
Solid lines always show Faddeev results and broken lines always Born results.

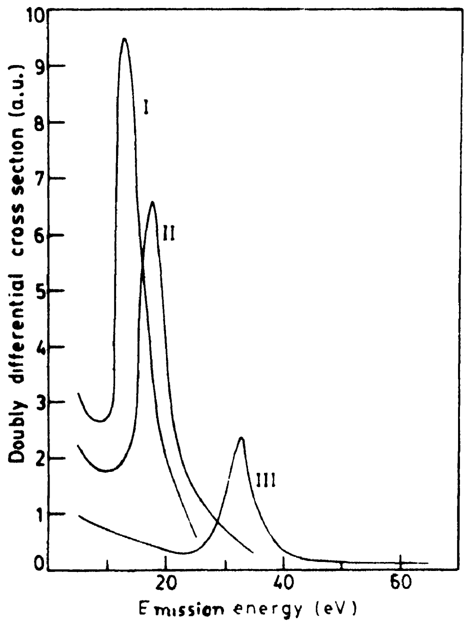

Figure 4. DDCS as a function of ejected electron energy, where $\theta_2 = 0°$ and
set I : $E_i = 40$ eV
set II : $E_i = 50$ eV
set III : $E_i = 80$ eV.

outgoing positron. The Born cross section, on the other hand, has relatively much smaller values than the Faddeev cross section near the forward direction, but grows higher to show a broad peak around $\theta = 45°$ at these energies.

B. Doubly differential cross section (DDCS) :

The forward doubly differential cross section when $\theta_2 = 0°$ is shown in Figures 4 and 5 as a function of the ejected energy E_2. We have computed these results at incident energies E_i = 40, 50, 80, 150, 300 and 500 eV. As found in our earlier calculation [1] at 43.2 eV for E_i = 100 eV, we now obtain cusps at energies $(E_i-13.6)/2$. These results indicate that there is an obvious asymmetry of the doubly differential cross section around the cusp peak at the energy $E_2 = E_1$. The fall rate of the cross section is much sharper at higher energies than its rise at lower energies. It is of further importance to note here that the cusp peaks are quite sharp at lower incident energies. As the energy is increased, the height of the peak is gradually decreased with the broadening of the width. For 300 eV positrons, there is only a low hump to be found as has been recently observed for Ar atoms by the University College, London group at 100 eV [17]. At 500 eV, the hump is almost flat.

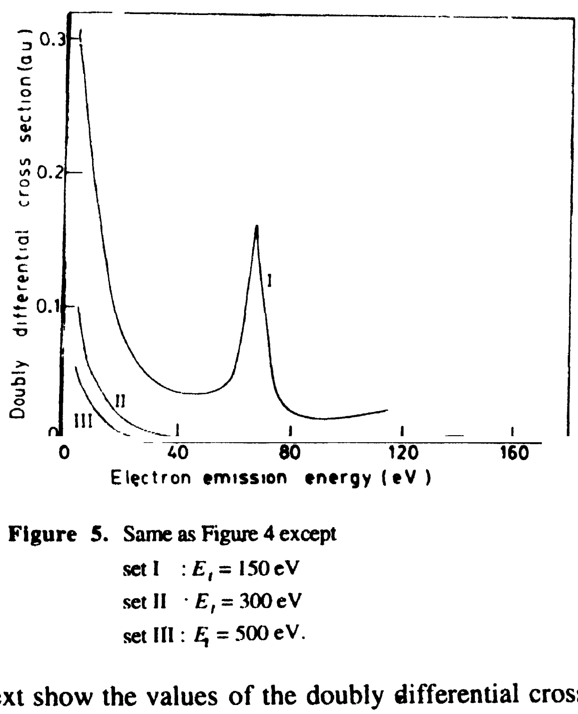

Figure 5. Same as Figure 4 except
set I : E_i = 150 eV
set II · E_i = 300 eV
set III : E_i = 500 eV.

We next show the values of the doubly differential cross section at θ_2 = 45° as a function of E_2 in Figure 6 for an incident positron energy 100 eV. In contrast to the behaviour at $\theta_2 = 0°$, the cross section for $\theta_2 = 45°$ as displayed in this figure does not show any rapid change in the whole emission energy range.

Finally two sets of results of the doubly differential cross section are presented in Figures 7–9. These are calculated as a function of the emission angle θ_2 (Figures 7, 8) and the scattering angle θ_1 (Figure 9) for electron energies 20 eV and 60 eV respectively at an incident positron energy 100 eV. The cross section $d^2\sigma/dE_2 d\theta_2$ obtained in the Born approximation shows a broad maximum at an intermediate emission angle for both these energies, while the corresponding Faddeev results fall from a forward peak smoothly to a minimum and then rises. For the other case in which we calculate $d^2\sigma/dE_2 d\theta_1$ as a function of θ_1, although the Faddeev results display a similar trend for both the emission energies,

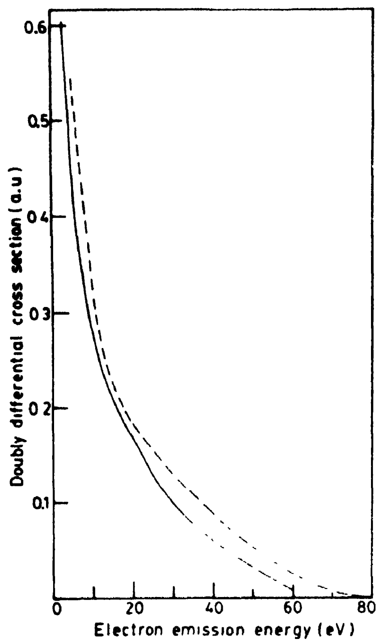

Figure 6. Same as Figure 4 except when E_i = 100 eV and θ_2 = 45°.

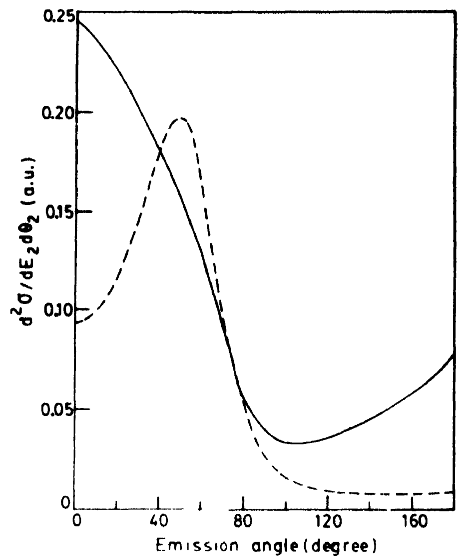

Figure 7. DDCS as a function of emission angles θ_2. Here E_i = 100 eV and E_2 = 20 eV.

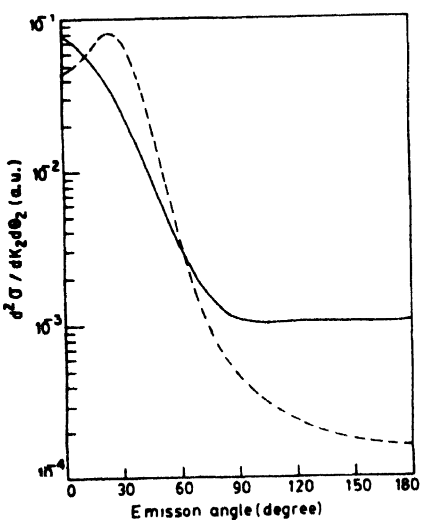

Figure 8. Same as Figure 7 except E_2 = 60 eV.

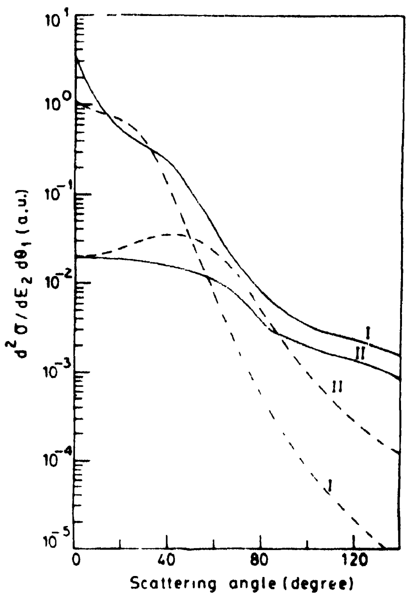

Figure 9. DDCS as a function of scattering angle θ_1 when E_i = 100 eV and
set I : E_2 = 20 eV
set II : E_2 = 60 eV.

there are some qualitative changes in the Born cross sections at these energies. The Born doubly differential cross section as reported here is found to be in agreement with that given in Mott and Massey [22].

4. Conclusion

Using the first-order wavefunction as given by Faddeev's three-body scattering formalism, we report here the triply differential cross sections in positron-atom collisions at intermediate and high energies for a number of asymmetric and symmetric geometries. In conformity with the findings of Schulz and Reinhold [13], we observe that the large angle behaviour of triple differential ionization cross section values are dominated by the capture to the continuum process. We have made a detailed study of the forward doubly differential cross section for several positron energies and obtained a cusp at lower energies less than 300 eV. At other emission angles for which the cusp conditions are not satisfied (*e.g.*, $|x_{21}|$ is not nearly zero), the cross section has a smooth behaviour as a function of the emission energy. An experimental verification of these theoretical predictions for positron-hydrogen system will be of utmost importance in view of the recent observations. Since these are first-order calculations, the present results of the triply and doubly differential cross sections should be basically valid at intermediate and high energies of positron impact.

References

[1] P Mandal, K Roy and N C Sil *Phys. Rev.* **A33** 756 (1986)

[2] L D Faddeev *Zh. Exsp. Teo. Fiz.* **39** 1459 [*Sov. Phys. JETP* **12** 1014] (1961)

[3] A Salin *J. Phys.* **B2** 631 1225 (1969)

[4] J Macek *Phys. Rev.* **A1** 235 (1970)

[5] R Shakeshaft and L Spruch *Phys. Rev Lett.* **4** 1034 (1978)

[6] C R Garibotti and J E Miraglia *Phys. Rev.* **A21** 572 (1980)

[7] R O Barrachina and C R Garibotti *Phys. Rev.* **A28** 1821 (1983)

[8] G B Crooks and M E Rudd *Phys. Rev Lett* **25** 1599 (1970)

[9] M W Lukas and K G Harrison *J. Phys.* **B5** L20 (1972)

[10] C R Vane, I A Sellin, M Sueter, G D Alton, S B Elston, P M Griffin and R S Theo *Phys. Rev. Lett.* **40** 1020 (1978)

[11] M W Lukas, K F Man and W Steckelmacher *Lecture Notes in Physics* **Vol. 213** eds K O Groenveld, W Meckback and I A Sellin (Berlin : Springer) p 1 (1984)

[12] M Brauner and J S Briggs *J. Phys.* **B19** L325 (1986)

[13] D R Schultz and C O Reinhold *J. Phys.* **B23** L9 (1990)

[14] M Brauner, H Klar and J S Briggs *J. Phys* **B22** 2265 (1989)

[15] A Roy, K Roy and N C Sil *J Phys* **B13** 3443 (1980), **B15** 1289 (1982)

[16] C J Joachain *Positron Scattering in Gases* eds by J W Humberston and M R C McDowell (New York : Plenum) p 39 (1983)

[17] J Moxom, G Laricchia, M Charlton, G O Jones and A Kover *J Phys* **B25** L613 (1992)

[18] M R C McDowell and J P Coleman *Introduction to Ion-atom Collisions* (Amsterdam : North-Holland) p 239 (1970)

[19] H S W Massay and C B O Mohr *Proc. Roy. Soc. (London)* **A140** 613 (1933)

[20] L D Landau and E M Lifshitz *Quantum Mechanics, Non-relativistic Theory* (London : Pergamon) 3rd edn. p 628 (1977)

[21] Ref. 18, p 322 and p 364

[22] N F Mott and H S W Massey *Theory of Atomic Collisions* (London . Pergamon) 3rd edn. p 490 (1965)

Appendix

On using the expression for V_2 in eq. (13), we obtain $J(\boldsymbol{R}_{21})$ in the form

$$J = \int \exp\left(-\lambda_i R_{23} + i\boldsymbol{Q}_2 \cdot \boldsymbol{R}_{23}\right) \left|\boldsymbol{R}_{23} - \boldsymbol{R}_{21}\right|^{-1} d\boldsymbol{R}_{23}. \tag{A1}$$

We now take the Fourier integral transforms of the quantities $\exp\left(-\lambda_i R_{23}\right)$ and $\left|\boldsymbol{R}_{23} - \boldsymbol{R}_{21}\right|^{-1}$, and then use the δ-function property to carry out the integration over $d\boldsymbol{R}_{23}$. We get an expression for J which involves an auxiliary volume integral over $d\boldsymbol{q}$ as

$$J = \frac{4\lambda_i}{\pi} \int \exp\left(i\boldsymbol{q} \cdot \boldsymbol{R}_{21}\right) d\boldsymbol{q} \Big/ \left[q^2\left(\left|\boldsymbol{q} - \boldsymbol{Q}_2\right|^2 + \lambda_i^2\right)^2\right] \tag{A2}$$

Introducing the Feynman integral for parameters a, b where

$$\frac{1}{ab} = \int_0 \frac{dx}{\left[ax + b(1-x)\right]^2} \tag{A3}$$

to the denominators of the integrand in eq. (A2) with $a = \left|\boldsymbol{q} - \boldsymbol{Q}_2\right|^2 + \lambda_i^2, b = q^2$, we are able to reduce the integral over $d\boldsymbol{q}$ conveniently to a one-dimensional integral. The final expression for J is given by

$$J = -2\pi\lambda_i \int_0^1 x dx\, e^{i\boldsymbol{A} \cdot \boldsymbol{R}_{21}} \left(\frac{1}{\mu} \frac{\partial}{\partial \mu}\right) \frac{1}{\mu} e^{-\mu R_{21}} \tag{A4}$$

where

$$\boldsymbol{A} = -x\boldsymbol{Q}_2, \tag{A5}$$

$$\mu^2 = x\lambda_i^2 + x(1-x)\, Q_2^2. \tag{A6}$$